 503 Franklin Street, Denver, Colorado, 80218. 303-388-1778. TCoxDenver@aol.com

A BIOMATHEMATICAL MODEL OF HEMATOTOXICITY

Louis Anthony Cox, Jr.
Cox Associates
Denver, CO, USA

July, 1998 – Revised May, 1999

ABSTRACT

Pharmacodynamic models representing interactions among chemicals and cells can help to clarify how time patterns of administered dose affect risks of adverse health outcomes. This paper summarizes a model that predicts the effects of the myelotoxic and immunosuppressive drug cyclophosphamide (CP) on the hematopoietic (blood-forming) system. It consists of a set of physiological compartments representing hematopoietic progenitor cell, granulocyte-macrophage (GM)-committed stem cells, and more mature blood cells. These compartments are linked by nonlinear feedback control loops and are susceptible to first-order cell-killing kinetics from cytotoxic metabolites.

The model has been validated by testing its predictions against experimental and clinical data for blood cell counts following administration of CP to mice, dogs, and humans. It successfully explains apparent anomalies and patterns in previously published data, including the fact that smaller cumulative doses can cause larger hematotoxic responses. An intriguing prediction from the model is that sustained exposures to sufficiently small concentrations of myelotoxic agents may tend to provoke a protective response, increasing rather than decreasing the numbers of GM colony-forming units (CFU-GM) and early hematopoietic stem cells available to sustain hematopoiesis.

KEY WORDS: Hematopoiesis, myelotoxicity, cyclophosphamide, pharmacodynamics, mathematical modeling, biologically-based risk assessment

INTRODUCTION

Applied quantitative health risk assessment seeks to answer questions such as the following. Suppose that a risk manager must choose among risk mitigation options (a)-(d) for protecting workers from a potentially hazardous airborne chemical in a manufacturing plant:

(a) Reduce daily occupational exposure time from 8 hours to 4 hours.
(b) Reduce 8-hour average workplace concentration by 50%.
(c) Reduce weekly exposure from 5 days to 2.5 days.
(d) Reduce yearly exposure from 50 to 25 weeks per year.

Which option is most health-protective? By how much would each be expected to reduce the health risk due to occupational exposures? How well can these questions be answered without further specifying the options, e.g., how the 4 hours in option (a) are distributed within the work day, how the 25 weeks in option (d) are distributed within the year, and so forth? This paper shows how biomathematical, biologically motivated risk assessment models can address such questions.

Section 1 presents empirical evidence motivating the need for explicit dynamic models of dose-response relations. Using the chemotherapeutic and immunosuppressive drug cyclophosphamide (CP) as a detailed example, Section 2 develops a dynamic dose-response model for predicting and explaining cytotoxic effects of chemicals on bone marrow and blood cell populations. Section 3 presents new results on empirical validation of the model with human clinical data and experimental animal data. Section 4 discusses potential implications for risk assessment of chemical leukemogens.

WHY DYNAMIC DOSE-RESPONSE MODELS?

The need for explicit dynamic models in quantifying dose-response relations is often implicitly denied in applied risk assessments. Instead, dose metrics, such as cumulative exposure or cumulative dose per unit body weight or per unit surface area, are commonly used to equate the risks of very different exposure histories. Dose metrics are used to extrapolate risks from high to low doses and from one species and

strain to others. Uncertainties about the validity of the extrapolation are often equated to uncertainty about the most appropriate choice of dose metric.

In conjunction with another widely used assumption – that excess risk at sufficiently low doses increases in approximate proportion to the dose metric – the dose metric approach provides a simple, clear method for assessing the risk consequences of risk management options such as (a) - (d). For example, these principles imply that all four options reduce health risk equally at small concentrations. Different practitioners might debate which specific parametric risk model is most appropriate, e.g., logistic regression, probit, proportional hazards, linear relative risk, linear absolute risk, and so forth. Yet, the rank-ordering of risk management options and estimates of their relative quantitative efficiencies in reducing risk do not depend on such model differences. They are fully determined by the assumptions of a dose metric and approximate low-dose linearity. This may create an apparent consistency and robustness in the results of different specific parametric risk models, including all of those just listed, that is traceable to their common underlying methodological approach.

Despite its simplicity and robustness, the dose metric modeling framework is inconsistent with experimental data that permit it to be tested, for some chemicals of practical interest. Stop-exposure experiments, which expose different groups of animals to chemical carcinogens for different amounts of time, reveal results that seem to contradict the most basic tenets of applied risk assessments based on dose metrics. For example:

- Smaller cumulative doses may produce larger toxic and carcinogenic responses (e.g., Luke *et al.,* 1988a for benzene cytotoxic effects on erythrocytes in mouse bone marrow; Cox *et al.* 1996 for isoprene effects on tumors at multiple anatomic sites in mice).

- Relatively small increases in concentration can dramatically increase tumor incidence (e.g., Williams *et al.* 1993 for hepatocarcinogenesis; Melnick *et al.* 1990 for butadiene-induced lymphomas).

- Extending durations of exposure may have little or no impact on tumor risks (Cox *et al.* 1996 for isoprene-induced tumors at several anatomic sites).

- Sufficiently low exposure concentrations can have disproportionately small impacts, or even appear to have beneficial effects, prompting some investigators to speculate about biological hormesis (David and Srendsgaard 1990).

Table I illustrates some of these phenomena for isoprene. The following patterns are noteworthy.

- Doubling concentration (from 70 ppm to 140 ppm between exposure groups 3 and 5) increases liver adenomas from 0.29 to 0.44. But, doubling weeks of exposure (from 40 to 80 between exposure groups 3 and 4) does not increase risk significantly at any site, and even appears to reduce it. This observation is not explained by competing risks of death from toxicity, as animals tolerated these concentrations. Nor is it explained by saturation of carcinogenic response mechanisms, as higher concentrations produce much higher tumor yields. Thus, no *dose-response theory that predicts that risk increases with cumulative exposure provides a useful model for these data.*

- Quadrupling exposure concentration from 70 ppm to 280 ppm while quartering exposure duration from 80 weeks to 20 weeks unambiguously increases tumor risk (compare exposure groups 4 and 6), even though cumulative exposures are identical. Thus, *no risk model that uses cumulative exposure (area under curve, AUC) as a dose metric adequately describes these data.*

- At higher concentrations, doubling hours-per-day of exposure while halving weeks of exposure increases the risk of adenomas and liver carcinomas (compare exposure groups 10 and 11), even though cumulative exposures are identical.

- Liver and lung tumors (both adenomas and carcinomas) are only significantly elevated at concentrations above 70 ppm. In this data set, 140 ppm is the smallest concentration for which significant increases were observed.

Such observations challenge any dose-response model that uses a dose metric in which risk increases monotonically and/or symmetrically with exposure concentration and duration.

TABLE I: RESULTS OF A STOP-EXPOSURE EXPERIMENT FOR ISOPRENE IN MALE B6C3F1 MICE

Stop-exposure experiments for health end-points other than cancer show similar patterns. Genotoxic, cytogenetic, and cytotoxic responses are often sensitive to the time pattern of dose administration, rather than only to the AUC of administered dose (or of metabolites formed). For example, Table II summarizes experimental results for benzene, a relatively well-studied human leukemogen and animal carcinogen, for endpoints other than (and perhaps causally prior to) cancer. Benzene metabolites such as phenol, hydroquinone (HQ), and catechol synergize strongly in producing both cytogenetic and cytotoxic damage. Since carcinogenesis is often postulated to arise from the combination of genotoxic and cytotoxic effects (e.g., Farris *et al.* 1997 for benzene; Williams *et al*. 1993, for the hepatocarcinogen DEN, Monticello and Morgan 1994 for formaldehyde), it is not surprising that chemicals with strongly nonlinear dose-response patterns for genotoxic and cytotoxic effects may exhibit similar nonlinear patterns for tumors.

TABLE II: RESULTS ON BENZENE HEMATOTOXICIT9Y AND GENOTOXICITY

These examples demonstrate the need for dose-response models that do not satisfy the usual assumption that risk is an increasing function of a dose metric that combines exposure concentration and duration in a simple, monotonic, and perhaps symmetric way. The following sections investigate the potential of biologically motivated models, which attempt to simulate key dynamic aspects of adverse health effects, to obtain more realistic and useful predictions.

METHODS

To assess how well biologically motivated models can predict and explain phenomena such as those in Tables 1 and 2, we carried out the following three steps:

a) Constructed a dynamic simulation model of pharmacokinetics and cytotoxicity / cell kinetics for a well-studied leukemogen (CP). Mathematical models of pharmacokinetics and metabolism, hematopoiesis (blood formation), and hematotoxicity and myelotoxicity (blood-poisoning and marrow-poisoning) were based on previously published data and modeling efforts for CP, as described below. They were combined and implemented in a continuous simulation model using the ITHINK™ modeling environment (High Performance Systems, 1997).

b) Validated the model's predictions with data from several species and agents. Model parameters estimated primarily from canine data were used successfully to predict observed dynamic responses in humans, dogs, and mice exposed to CP. Interspecies extrapolations were made by adjusting only two scaling parameters – a time scaling factor and a dose scaling factor – to account for differences in body weight and metabolism. Similar work has recently validated similar model predictions for effects of radiation on human and canine hematopoiesis (Fliedner *et al.* 1996; Tibken and Hofer 1995).

c) Applied the validated model to explain and predict the dynamic responses of specific cell populations to different time patterns of dosing with hematotoxic agents. Dynamic responses were simulated for specific hematopoietic progenitor cell populations (e.g., early CFU-GM) thought to be involved in chemically induced myeloid leukemogenesis (Irons and Stillman 1996).

The methods used to carry out each step are described next.

STRUCTURE OF THE BIOLOGICALLY MOTIVATED MODEL

The biomathematical model of hematotoxicity is described in Cox (1996), which gives detailed model equations in an appendix. It is based on the model of Steinbach *et al.* (1980) with some simplifications and improved CP pharmacokinetics based on experimental data (Sladek 1988).

The model consists of the following components:

COMPARTMENTS

1. A simple *linear compartmental flow model* (Jacquez 1997) describes the pharmacokinetics and metabolism of CP in humans. The model structure and micro-constants describing CP pharmacokinetics and metabolism are based on measurements in human patients, which are well approximated by a classical two-compartment model (Cohen *et al.* 1971; Sladek 1988). Because pharmacokinetics and metabolism are approximately linear, the area-under-curve per unit time for any CP metabolite in any compartment is approximately proportional to the AUC-per-unit time of administered CP. This proportionality justifies using a simple classical compartmental model, since it is likely that a more realistic and sophisticated description of metabolism and pharmacokinetics (e.g., a PBPK model) would not noticeably change predictions for hematotoxic responses.

2. A *nonlinear compartmental flow model* with feedback-control loops, describing the myelotoxicity and hematotoxicity of CP. This model consists of the following six main sequential compartments, describing the granulocyte-macrophage (GM) lineage of the hematopoietic system:

    - Early stem cells and hematopoietic progenitor cells (HPCs)
    - Granulopoietic committed stem cells (e.g., CFU-GM)
    - Proliferative cells (myeloblasts, promyelocytes, myelocytes)
    - Maturation pool
    - Bone marrow reserve

- Peripheral blood granulocytes

Each compartment is fed by its predecessors and may provide feedback to them via control signals (e.g., representing the cytokine network). Partial differential equations (PDEs) describe the dynamics of the age-structured CFU-GM cell populations and later proliferative populations. The simulation model approximates these PDEs numerically by systems of ordinary differential equations ODEs (10 serial subcompartments), to make the mean and variance of cell transit times conform to experimentally observed values in dogs (Steinbach *et al.* 1980).

FEEDBACK CONTROL

Nonlinear feedback loops, implicitly modeling the regulatory effects of the cytokine network, feed back information (interpreted as strengths of regulatory signals) from blood cell population sizes to control the following rate parameters:

- Fraction of early HPCs that differentiate instead of self-renewing;
- Rate of recruitment of resting stem cells into active cycling;
- Birth rates of CFU-GM and downstream proliferative cells;
- Release rate of mature granulocytes from the bone marrow reserve to the peripheral blood.

These feedback control laws are described by smooth curves that were constructed to pass through experimental data points. Typically, the experimental data consisted of extreme values (e.g., maximal and minimal cell division rates observed under a variety of experimental conditions) with some intermediate data points. A parametric s-shaped function was then used to interpolate among these observed values, with its parameters being estimated by least squares. Most of the parameter values for the CP cytotoxicity and cell kinetics component were taken from previously published estimates based on a model of granulopoiesis in dogs (Steinbach *et al.* 1980). See the appendix of Cox (1996) for details of the functions and parameter values used.

SIMULATION FRAMEWORK

The combined CP pharmacokinetics and hematotoxicity model is a continuous simulation model of the standard form (e.g., van der Bosch and van der Klauw 1994):

$$d\mathbf{x}(t)/dt = \mathbf{f}[\mathbf{x}(t), \mathbf{b}(t)]$$
$$\mathbf{b}(t) = \mathbf{g}[\mathbf{x}(t)]$$

where **x**(t) is a state vector with components describing (a) the quantity of CP and its metabolites in each compartment of the pharmacokinetic model and (b) the number of cells in each compartment of the cell kinetics and cytotoxicity model at time t. **b**(t) is a vector of rate parameters. Its components are constants for the pharmacokinetic model and are functions of the cell population sizes for the cell kinetics and cytotoxicity model. **b**(t) also includes cytotoxic parameters describing the rate of cell-killing of cycling HPCs and CFU-GM cells per unit concentration of toxic CP metabolites (specifically, phosphoramide mustard) in these marrow cell populations. The feedback laws determining **b**(t) from **x**(t) are symbolized by the vector function **g** and are detailed in Cox (1996). Initial values for cell population sizes were taken from published experimental data, as in Steinbach *et al.* (1980), and starting values for CP in different compartments were assumed to be zero. Given the initial conditions **x**(0) and any specified dosing history, the simulation model determines the resulting histories of CP and metabolite concentrations and fluctuations in hematopoietic cell populations by numerical integration of the simulation model equations.

MODEL VALIDATION METHODS

We validated the biologically motivated hematotoxicity model for CP by comparing its predictions to data not used in creating the model. The empirical validation consisted of the following two efforts:

- *Validation in humans:* Using the model formulated above for dogs and a simple adjustment for interspecies dose conversion, we predicted the effects of repeated CP treatments on humans. We compared the model predictions to published clinical data to assess its predictive validity for humans.

- *Validation in mice*: Using the above model and the same simple adjustment for interspecies dose conversion, we predicted the effects on hematopoiesis (CFU-GM and peripheral granulocytes) of single- and multiple injections of CP in mice. The predictions were tested by carrying out these experiments.

Fliedner *et al.* (1996) and Tibken and Hofer (1995) have also validated a closely similar model for radiation effects on hematopoiesis in dogs and humans.

INTERSPECIES EXTRAPOLATION

The model of Steinbach *et al.* (1981) was developed for dogs, for which it appeared to have useful descriptive validity. To test the validity of our modified model, we compared its predictions against experimental observations in mice and humans.

Since humans have a larger body weight than dogs, their physiological processes are expected to run more slowly. The most parsimonious way to adjust for this effect is to dilate the time axis, multiplying it by a constant greater than 1 to slow down predicted canine hematotoxic responses (e.g., changes in cell population sizes) to predict the timing of corresponding human responses. Rather than using allometric arguments to estimate the scaling factor, we estimated it directly by comparing the results of analogous experiments in dogs and humans. Comparing the time course of peripheral white blood cells (WBCs) in canine model simulations following a single injection of CP (Steinbach *et al.* 1980) to the time course reported for humans (Coggins *et al.* 1960) showed that the nadir occurs at approximately 11 days in humans compared to approximately 7.5 days in dogs. Thus, predictions from the canine model are scaled by a factor of 11/7.5 = 1.47 along the time axis to obtain predictions for humans. The pharmacokinetics submodel is already developed from human data (Cohen 1971), and hence requires no rescaling. Also, rescaling its relatively fast dynamics would make

little or no difference to the slower CP-hematotoxicity submodel for most dosing scenarios.

For mice, a contraction of the time axis must be made. Comparing experimental data on murine hematotoxic responses to CP injections (DeWys *et al.* 1970) to human clinical data (Bergsagel *et. al*., 1968; Buckner *et al.* 1972; Nissen-Meyer and Host 1960) suggested that the time scale for hematopoietic responses in mice should be contracted by a factor of about 0.4 compared to humans. This estimated adjustment factor was used in making all predictions for mice.

Mice have a higher ratio of surface area-to-volume than do dogs or humans. Therefore, the administered mg/kg required to produce a given dynamic response in mice (e.g., a given depth of the nadir as a percentage of the normal level) may be different from the mg/kg required to produce the same response in dogs or humans. The required dose-scaling factor was estimated very approximately as about 5, based on the observation that mouse responses to 300 mg/kg (DeWys 1970) appear to correspond roughly to human responses to 60 mg/kg (Coggins *et al*. 1960), appropriately speeded up. However, responses within each species to all sufficiently high single doses are similar enough to each other so that the exact correspondence between mouse and human dose scales is hard to identify from previously published data. (While it might in principle be desirable to also account for differences between dogs and humans in the hematotoxic potency of CP, the high levels of CP used in clinical trials approximately saturate the hematotoxic response, making detailed potency adjustments unnecessary.)

MODEL VALIDATION TESTS

The complete CP model contains over 120 individual equations and formulas and over 20 parameter values, all with values estimated from experimental data. To validate its assumptions and implications, we took the following steps.

Face validity and internal consistency of the model were tested by introducing deliberate errors into its equations (e.g., using incorrect formulas or parameter values) and confirming that the resulting outputs became unrealistic, e.g., unstable in the absence of any external perturbation from dosing. These efforts revealed that the self-consistent dynamic behaviors exhibited by the model (specifically, homeostasis and a stable

steady state) do not survive introduction of such obvious errors, increasing confidence that they have not been made.

Descriptive validity of the original Steinbach *et al.* model was established by checking that its predictions for HPC stem cells in bone marrow and for WBC counts after an injection of 15 mg/kg CP agree with experimental observations on dogs (Steinbach *et al.* 1980). These same experimental data points had been used to estimate the model parameters, however, so this check only confirms the descriptive validity of the model, i.e., its ability to explain a large number (over 70) data points with a much smaller number of parameters. It does not prove that other parameter values would not fit the same experimental data equally well but make different predictions outside the range of observed experimental conditions.

Predictive validity of the CP model was first assessed using human data by simulating the outcomes of clinical experiments previously reported in the literature (Buckner *et al.* 1972; Nissen-Meyer and Host 1960) and comparing the model-predicted time courses of blood cell counts to corresponding clinically observed values. The human data sets and clinical trials used to test the model are quite different from the animal experiment data sets used to build it, thus providing a fair test of its ability to make useful predictions across these species and experimental conditions.

The model's predictive validity was further tested through new experiments in male B6C3F1 mice, conducted at the University of Colorado Medical School in Denver by Drs. R. Irons and W. Stillman. Table III summarizes the experimental design used. Five mice were sacrificed at each "x" and 50 mg/kg of CP was administered by i.p. injection into surviving mice at each "D". Rows 1-3 represent three treatment groups, receiving one, two, and three doses of CP, respectively, spaced 48 hours apart. Row 0 is the control group. This design was constructed based on simulation model results, which predicted large, testable differences in CFU-GM population sizes on different days for these three dose regimens.

A pilot experiment consisting of a single injection on day 1 and a one-week follow-up with sacrifices on days 2, 4, and 7 confirmed that mice could tolerate 50 mg/kg and that CFU-GM and WBC counts looked as predicted on these days. Mice were sacrificed by cervical dislocation and bone marrow was extracted, plated, and assayed for CFU-GM stem cells using a colony-forming assay.

TABLE III: DESIGN OF MODEL VALIDATION EXPERIMENT IN MICE

RESULTS

Following the validation tests, the biologically motivated hematotoxicity model was applied to several dose scenarios to determine whether it could help to explain the phenomena in Tables 1 and 2. Scenarios examined included:

1. Stop-exposure experiments, similar to those for isoprene and benzene in Tables 1 and 2, that allocate the same total administered dose according to different time patterns to determine which create the largest predicted hematotoxic effects on CFU-GM populations.

2. Continuous infusion experiments, intended to create internal dose profiles similar to those that might arise from sustained low-level exposures to an air-borne leukemogen such as benzene.

The model-based predictions for these dosing scenarios were used to draw inferences about dose-response relations that may help to explain some of the qualitative patterns noted in Tables 1 and 2 for other chemicals and end-points.

RESULTS OF MODEL VALIDATIONS FOR HUMANS

Buckner *et al*., (1972) report clinical data for nine human cancer patients administered 60 mg/kg of CP each via infusion, and for seven patients each given 120 mg/kg CP as two 60 mg/kg infusions spaced one day apart. The CP model was used to predict the time courses of WBCs for these groups of patients. Figure 1 shows the model predictions and the observed data for both groups. The results from the simulation model provide a useful approximation to the empirically observed results. In both the simulation and the clinical data, the WBC time courses are not significantly different between the 60 mg/kg and the 120 mg/kg groups for the first week following exposure. They begin to separate in the second week, with severe leukopenia persisting for over 4 days in the 120 mg/kg group before noticeable recovery begins, compared to an earlier recovery in the 60 mg/kg group. This match between predictions and observations is reassuring, especially considering that the model was developed

using canine data. Model predictions match observed data similarly well throughout the duration of observations for a clinical trial in which CP was administered on four consecutive days (Nissen-Meyer and Host 1960).

FIGURE 1: MODEL PREDICTIONS *vs.* CLINICAL OBSERVATIONS FOR TWO ADMINISTERED DOSES (60 AND 120 MG/KG OF CP)

.

OBS = observed values; PRED = model-predicted values

RESULTS OF VALIDATION EXPERIMENTS IN MICE

Figures 2a and 2b present the main results of the validation experiments in mice. Figure 2a shows predicted *vs.* actual results for CFU-GM time courses in a single-injection pilot experiment. (Peripheral granulocyte-macrophage counts were also predicted, and provide even better matches to observed values than CFU-GM. Since the bone marrow CFU-GM responses are both more volatile and hence harder to predict, they are the focus of this summary.) Figure 2b shows the outcome of the multiple-injection experiment described in Table III. The three panels, a, b, and c, show the observed (squares) and predicted (circles) average values of CFU-GM for mice sacrificed on different days in each of the three treatment groups. (Straight-line extrapolations and interpolations are sketched among the data points. In the middle panel, for dose group 2, these segments are not connected for days 5 and 6 because their locations are uncertain.) Mean values of CFU-GM counts among all animal sacrificed in each treatment group on each sacrifice day are shown. All plotted values are expressed relative to the control group values, i.e., 1 is the no-effect level.

There is enough experimental variability between replicates so that an exact match between predicted and observed values would not be expected in any single experiment. For example, the left-most panel of Figure 2b repeats the single-injection dose regimen in Figure 2a, yet produces a different time course of observed relative CFU-GM counts in bone marrow. However, the predicted time courses are similar to the observed ones in approximate magnitudes and timings of changes in CFU-GM

counts. The largest discrepancies (e.g., at the left ends of the curves in Figure 2b) occur when the CFU-GM compartment is predicted to be most volatile, with population sizes changing dramatically from hour to hour. (Indeed, the experiment design in Table III was chosen to produce just such, large, fast variations so that they could easily be detected.) There is rough agreement between predicted and observed values in terms of magnitude, direction of change, and approximate timing of peaks and of recovery (starting to return to pre-exposure levels), despite the experimental variability.

The model validation results in Figures 1 and 2 suggest that the simulation model of hematotoxicity may provide useful approximate predictions in novel situations, especially for humans but less so for mice. This suggestion is strengthened by independent investigations of other researchers (Fliedner *et al.* 1996; Tibken and Hofer 1995), who also used an outgrowth of the Steinbach *et al.* (1980) model to predict CFU-GM responses in dogs and humans exposed to radiation. Their results and the new model validation experiments reported above provide empirical support for applying the simulation model to predict CFU-GM and peripheral granulocyte-macrophage responses to situations for which data are not yet available.

FIGURE 2a: Predicted vs. Actual CFU-GM Values In Mice After One CP Injection

FIGURE 2b: Predicted vs. Actual CFU-GM Values In Mice After One, Two, and Three CP Injections

RESULTS OF MODEL APPLICATIONS

Figure 3 examines the predicted effects of repeated infusions of CP, selected to roughly mimic the experimentally observed GM-lineage effects of two different concentrations of benzene inhaled for 6 hours/day for different amounts of time (Green *et al.* 1981). The exposure corresponding to 10 ppm for 10 weeks (or more) has only a relatively small predicted effect on mouse bone marrow CFU-GM (curve 2). Yet, an algebraically equal (or smaller) exposure of 100 ppm for 6 hours/day for 1 week has a

much larger predicted effect on CFU-GM (curve 1), as measured by depth of nadir and height of zenith. Such predictions agree with and may help to explain experimental observations (e.g., Green *et al.* 1981).

Other simulation experiments produced the following conclusions:

- *A dose of CP administered over 8 hours creates a larger hematotoxic effect than the same dose administered over 120 or 480 hours,* as measured by depth of nadir or maximum height of the recovery curve of CFU-GM. The 8-hour administration leads to a profound initial depression in CFU-GM cells, followed by a rapid rebound and overshoot as a result of compensating proliferation. Such a pattern might create a higher risk of leukemia than the other dosing scenarios if the proliferation amplifies a population of stem cells that has just been enriched with early HPCs (Irons and Stillman, 1996).

- *Doubling the duration of exposure from 240 hours to 480 hours less than doubles the simulated hematotoxic response.* In effect, the hematopoietic system is able to partially recover during exposure (provided that the dose rate is small enough to be tolerated without driving CFU-GM toward zero). During sustained dosing at low concentration levels, the number of early CFU-GM cells approaches a stressed-equilibrium level that is somewhat higher than normal. The nadir during the initial transient response is not very low (i.e., the normal stem cell population is not much depleted) and the recovery period is comparatively lengthy. Thus, the post-dosing proliferation may be expected to occur in a population that has not been as greatly enriched with at-risk stem cells as in the 8-hour dosing scenario. Indeed, if repair or elimination of inappropriately recruited stem cells and their progeny takes place at a fast enough rate, then the 240-hour exposure (leading to a zenith of proliferation about two weeks after dosing begins) might plausibly be more risky than the 480-hour exposure.

- *Hematotoxic response (e.g., as indicated by height of zenith) is not a simple monotonic function of administered concentration*. For example, suppose that dosing is continued until a steady-state equilibrium is reached. If the dose rate (e.g., administered concentration) is sufficiently small, then the predicted equilibrium size of the CFU-GM pool is greater than in the absence of dosing and it increases as

dose rate increases. At higher concentrations, however, the CFU-GM pool size falls below its normal unstressed level and decreases further as dose rate increases.

If other organ systems and stem cell populations undergo similar feedback control processes in responding to chemical carcinogens, then similar qualitative characteristics might be expected for the dynamic dose-response relations.

Table IV summarizes recent findings for several chemicals that suggest the following common pattern: When cytotoxicity-mediated cell proliferation plays an essential role in experimentally observed carcinogenesis, the dose-response pattern is typically non-linear at low doses and may exhibit hormesis.

The model described in this paper offers a detailed explanation/prediction of this pattern in terms of the predicted dynamics of bone marrow stem cell (CFU-GM) responses to myelotoxic agents such as CP.

TABLE IV: RECENT EVIDENCE ON CYTOTOXICITY AND DOSE-RESPONSE RELATIONS FOR SEVERAL CHEMICALS

CONCLUSIONS

The time patterns of hematopoietic responses generated by the CP model predict several phenomena that are inconsistent with simpler dose-response models but that occur in practice. These include

- Responses that increase less than proportionally when exposure durations are increased, while holding administered concentration constant.

- Nonmonotonic relations between concentration and response, suggesting that the relation between concentration and response may be different at very low concentrations than it is at higher concentrations.

- Response patterns that depend not only on the total dose (AUC of administered dose), but also on how the it is administered over time. Specifically, reducing exposure duration while proportionally adjusting exposure concentration can lead to

larger responses (deeper nadir, higher and quicker zenith) for the same total administered doses.

These simulated phenomena are consistent with some of the complexities observed in real dose-response patterns from stop-exposure experiments, as mentioned in the introduction.

These results suggest possible explanations for the apparent anomalies noted in Tables 1 and 2, including the fact that larger cumulative doses may create smaller effects. The explanation relies on the nonlinearity of stem cell dynamics in response to cytotoxic stresses. Although the CP model is specific to hematopoietic cell populations and leukemogenesis, it is tempting to speculate that similar nonlinear dynamics and feedback control loops may help to explain the observed anomalies in other experimental systems, such as those in Table IV.

In addition to predicting specific response patterns, the CP model provides potentially useful qualitative insights into the dynamics of hematopoietic responses. For example, simulation experiments in which two doses are separated by different amounts of time show that the hematopoietic system response smooths rapid transients in exposure inputs. In other words, it responds slowly enough (on a time scale of days to weeks) so that doses spaced closely (hours to a day or two apart) create essentially the same impact as a single combined dose. Thus, for example, if it is desired to keep both the depth of the initial nadir of WBCs and the height of the subsequent peak small, then increasing the duration of the recovery period between the two successive doses from 1 day to 4 days would make relatively little difference. Allowing a week or 10 days instead of 4 days between successive doses would make a relatively large difference. Similarly, options (a) and (b) in the example at the beginning of this paper are expected to have a larger impact than options (c) and (d).

In summary, the type of dynamic dose-response model developed here for CP may help to design exposure regulations and guidelines protect human health more effectively than standards based on AUC or concentration. Guidelines that take into account the importance of exposure timing might be less burdensome than some current standards that assume (incorrectly, if the simulation experiments reported here are an accurate guide) that long-duration, low-concentration exposure scenarios are "equivalent" in risk to brief, high-concentration exposures. The dynamic simulation

approach described in this paper can help to quantify the extent to which realistic dynamic dose-response patterns are likely to differ from those predicted by simpler dose-metric models.

REFERENCES

Barale R.; Marrazzini A.; Betti C.; Vangelisti V.; Loprieno N.; Barrai I. Genotoxicity of two metabolites of benzene: phenol and hydroquinone show strong synergistic effects in vivo. Mutation Research May;244(1):15-20; 1990.

Battelle Pacific Northwest Laboratories. Two-Year Chronic Inhalation Toxicity Study of 1,3-Butadiene in Mice. Report to the National Toxicology Program. Richland, WA. 1989.

Bergsagel, D.E., Robertson, G.L.; Hasselback, R. Effect of cyclophosphamide on advanced lung cancer and the hematological toxicity of large, intermittent intraveneous doses. Canadian Medical Association Journal. 98:532-538; 1968.

Buckner, C.D.; Rudolph, R.; Fefer, A.; Clift, R.A.; R.B. Epstein, R.B.; Funk, D.D.; Neiman, P.E.; Slighter, S.J.; Storb, R.; Thomas, E.D. High-dose cyclophosphamide therapy for malignant disease: Toxicity, tumor response, and the effects of stored autologous marrow. Cancer. 29:357-365; 1972.

Butterworth, BE.; Larson, J.L.; Conolly, R.B.; Borghoff, S.J.; Kedderis, G.L.; Wolf, D.C. Risk assessment issues associated with chloroform-induced mouse liver tumors. CIIT Activities 14:2; 1994.

Calabrese, E.J.; Baldwin, L.A.; Mehendale. H.M. G2 subpopulation in rat liver induced into mitosis by low-level exposure to carbon tetrachloride: An adaptive response. Toxicology and Applied Pharmacology. 121:1-7; 1993.

Chen, H.; Eastmond, D.A. Synergistic increase in chromosomal breakage within the euchromatin induced by an interaction of the benzene metabolites phenol and hydroquinone in mice. Carcinogenesis, 16(8):1963-1969; 1995.

Chen, H.; Rupa, D.S.; Tomar, R.; Eastmond, D.A. Chromosomal loss and breakage in mouse bone marrow and spleen cells exposed to benzene in vivo. Cancer Research. 54:3533-3539; 1994.

Ciranni R.; Barale R.; Adler ID. Dose-related clastogenic effects induced by benzene in bone marrow cells and in differentiating spermatogonia of Swiss CD1 mice. Mutagenesis. 6(5):417-421; 1991.

Clewell H.J.; Gentry P.R.; Gearhart J.M.; Allen B.C.; Andersen M.E.; Considering pharmacokinetic and mechanistic information in cancer risk assessments for environmental contaminants: examples with vinyl chloride and trichloroethylene. Chemosphere. 31(1):2561-2578; 1995.

Coggins, P.R.;.Ravdin R.G.; Eisman, S.H. Clinical evaluation of a new alkylating agent: Cytoxan (Cyclophosphamide). Cancer. 13:1254-1260; 1960.

Cohen L.L.; Jao, J.Y.; Jusko, W.J. Pharmacokinetics of cyclophosphamide in man, British Journal of Pharmacology. 43: 677-68; 1971.

Cox, L.A., Jr.; Bird, M.G.; Griffis, L. "Isoprene cancer risk and the time pattern of dose adminstration." Toxicology. 113:263-272; 1996.

Cox, L.A., Jr., Reassessing benzene risks using internal doses and Monte-Carlo uncertainty analysis. Environmental Health Perspectives. 104:Supplement 6, December, 1996.

Cronkite E.P.; Drew R.T.; Inoue T.; Hirabayashi Y.; Bullis J.E.; Hematotoxicity and carcinogenicity of inhaled benzene. Environmental Health Perspectives. 82:97-108; 1989.

David, J.M.; and Srendsgaard, D.J.; "U-shaped dose-response curves: Their occurrence and implications for risk assessment." J. Toxicology and Environmental Health. 30:71-83; 1990.

DeWys, W.D.; Goldin, A.; Mantel N. "Hematopoietic recovery after large doses of cyclophosphamide: Correlation of proliferative state with sensitivity: Cancer Research. 30:1692-1697; 1970.

Farris G.M.; Wong V.A.; Wong B.A.; Janszen D.B.; Shah R.S. Benzene-induced micronuclei in erythrocytes: an inhalation concentration-response study in B6C3F1 mice. Mutagenesis. Sep;11(5):455-462; 1996.

Farris G.M.; Robinson S.N.; Gaido K.W.; Wong B.A.; Wong V.A.; Hahn W.P.; Shah R.S.; Benzene-induced hematotoxicity and bone marrow compensation in B6C3F1 mice. Fundam Appl Toxicol. 36(2):119-129;1997.

Fliedner T.M.; Tibken B.; Hofer E.P.; Paul W. Stem cell responses after radiation exposure: A key to the evaluation and prediction of its effects. Health Phys (G2H). 70 (6):787-97;1996.

Golden R.J.; Holm S.E.; Robinson D.E.; Julkunen P.H.; Reese E.A.;. Chloroform Mode of Action: Implications for Cancer Risk Assessment. Regul Toxicol Pharmacolt. 26(2):142-155;1997.

Green, J.D.; Snyder, C.A.; LoBue, J, ; Goldstein, B.D.; Albert, R.E. Acute and chronic dose/response effect of benzene inhalation on the peripheral blood, bone marrow, and spleen cells of CD-1 male mice. Toxicology and Applied Pharmacology. 59:204-214; 1981a.

Green, J.D.; Snyder, C.A.; LoBue, J, ; Goldstein, B.D.; Albert, R.E. Acute and chronic dose/response effect of inhaled benzene on multipotential hematopoietic stem (CFU-S) and granulocyte/macrophage progenitor (GM-CFU-C) cells of CD-1 male mice. Toxicology and Applied Pharmacology. 59:204-214; 1981b.

Guy R.L.; Dimitriadis E.A.; Hu P.D.; Cooper K.R.; Snyder R. Interactive inhibition of erythroid 59Fe utilization by benzene metabolites in female mice. Chem Biol Interact. 74(1-2):55-62;1990.

Irons, R.D.; Stillman, W.S.; Colagiovanni, D.B.; Henry, V.A. "Synergistic action of the benzene metabolite hydroquinone on myelopoietic stimulating activity of granulocyte/macrophage colony-stimulating factor in vitro," Proceedings of the National Academy of Sciences USA. 89:3691-3695; 1992.

Irons R.; Stillman, W. The process of leukemogenesis. Environmental Health Perspectives. 104, Supplement 6, December:1239-1247; 1996.

Jacquez, J.A. Compartmental Analysis in Biology and Medicine, 3rd Edition. Wiley, 1997.

List, A.F.; Jacobs, A. Biology and pathogenesis of the myelodysplastic syndromes. Seminars in Oncology. 19(1):14-24; 1992.

Luke, C.A.; Tice, R.R.; Drew, R.T.; The effect of exposure regimen and duration on benzene-induced bone marrow damage in mice. I. Sex comparison on DBA/2 mice. Mutation Research. 203:251-272; 1988a.

Luke, C.A.; Tice, R.R.; Drew, R.T.; The effect of exposure regimen and duration on benzene-induced bone marrow damage in mice. II. Strain comparisons involving B6C3F1, C57Bl/6 and DBA male mice. Mutation Research. 203:273-295; 1988b.

Lutz U.; Lugli S.; Bitsch A.; Schlatter J.; Lutz W.K.; Dose Response for the Stimulation of Cell Division by Caffeic Acid in Forestomach and Kidney of the Male F344 Rat. Fundam Appl Toxicol. 39(2):131-137; 1997.

Lutz W.K. Dose-response relationships in chemical carcinogenesis: from DNA adducts to tumor incidence. Adv Exp Med Biol. 283:151-156; 1991.

Marrazzini A.; Chelotti L.; Barrai I.; Loprieno N.; Barale R. In vivo genotoxic interactions among three phenolic benzene metabolites. Mutation Research. 341(1):29-46; 1994.

Melnick, R.L.; Huff, J.E.; Roycroft, J.H.; Chou, B.J.; Miller, R.A. "Inhalation toxicology and carcinogenicity of 1,3-butadiene in B6C3F1 mice following 65 weeks of exposure". Environmental Health Perspectives. 86:27-36; 1990.

Monticello T.M.; Morgan K.T. Cell proliferation and formaldehyde-induced respiratory carcinogenesis. Risk Analysis.14(3):313-319; 1994.

Monticello T.M.; Swenberg J.A.; Gross E.A.; Leininger J.R.; Kimbell J.S.; Seilkop S.; Starr T.B.; Gibson J.E.; Morgan K.T.; Correlation of regional and nonlinear

formaldehyde-induced nasal cancer with proliferating populations of cells. Cancer Res 1. 56(5):1012-1022;1996.

Moolgavkar, S.; Dewanji, A.; Venzon, D.J. A stochastic two-stage model for cancer risk assessment. I. The hazard function and the probability of tumor. Risk Analysis. 8(3): 383-392; 1988.

Nissen-Meyer R.; Host H.; Kjellgren K.; Mansson B.; Norin T. Short perioperative versus long-term adjuvant chemotherapy. Recent Results Cancer Res. 98:91-98; 1985.

Portier, C.J. Utilizing biologically based models to estimate carcinogenic risk. In S.H. Moolgavkar (ed), Scientific Issues in Quantitative Cancer Risk Assessment. Birkhauser. Boston. 1990.

Robertson M.L.; Eastmond D.A.; Smith M.T.; Two benzene metabolites, catechol and hydroquinone, produce a synergistic induction of micronuclei and toxicity in cultured human lymphocytes. Mutat Res. 249(1):201-209;1991.

Scheding, S.; Loeffler, M.; Schmitz, S.; Seidel, H-J.; Wichmann, H.E. Hematoxic effects of benzene analyzed by mathematical modeling. Toxicology. 72:265-279; 1992.

Steinbach, K.H.; Raffler, H.; Pabst, G.; Fliedner, T.M. "A mathematical model of canine granulocytopoiesis". Journal of Mathematical Biology. 10:1-12; 1980.

Steinberg; DeSesso. Regul Toxicol Pharmacol.18:137-153; 1993.

Sladek, N.E. Metabolism of oxazaphosphorines. Pharmacology and Therapeutics. 37: 301-355;1988.

Tibken B.; Hofer E.P. A biomathematical model of granulocytopoiesis for estimation of stem cell numbers. Stem Cells. 13: 283-289; 1995.

Tice R.R.; Luke C.A.; Drew R.T. Effect of exposure route, regimen, and duration on benzene-induced genotoxic and cytotoxic bone marrow damage in mice. Environ Health Perspect. 82:65-74;1989.

Valberg, P.A.; Watson, A.Y. Analysis of diesel-exhaust unit-risk estimates derived from animal bioassays. Regulatory Toxicology and Pharmacology. 24:30-44;1996.

Toft, K.; Olofsson, T.; Tunek, A.; Berlin, M. Toxic effects on mouse bone marrow caused by inhalation of benzene. Archives of Toxicology. 51:295-302; 1982.

van der Bosch, P.P.J.; van der Klauw, A.C. Modeling, Identification, and Simulation of Dynamical Systems. CRC Press. Boca Rotan, Florida. 1994.

Williams, G.M.; Gebhardt, R.; Sirma, H.; Stenback, F. "Non-linearity of neoplastic conversion induced in rat liver by low exposures to diethylnitrosamine." Carcinogenesis.14(10):2149-2156; 1993.

Tables, in order of appearance

TABLE I: RESULTS OF A STOP-EXPOSURE EXPERIMENT FOR ISOPRENE IN MALE B6C3F1 MICE

Group	*ppm*	*weeks*	*hr/day*	*Liver adenomas*	*Lung Adenomas*	*Other adenomas*	*Liver carcinomas*	*Lung carcinomas*	*Histio-sarcomas*
1	*0*	*0*	*8*	0.22	0.22	0.14	0.18	0	0
2	*10*	*80*	*8*	0.24	0.32	0.12	0.12	0.02	0.04
3	*70*	*40*	*8*	0.29	0.16	**0.30***	0.22	0	0.04
4	*70*	*80*	*8*	0.30	0.08	0.18	0.18	0.04	0.04
5	*140*	*40*	*8*	**0.44***	0.20	**0.28***	0.20	0.02	0.02
6	*280*	*20*	*8*	0.36	0.32	**0.36***	0.24	0.06	**0.16***
7	*2200*	*80*	*4*	**0.42***	0.30	**0.56***	0.30	0.06	**0.14***
8	*2200*	*40*	*8*	**0.57***	**0.59***	**0.65***	**0.37***	0.06	**0.14***

Explanation: Columns 2-4 summarize the exposure factors defining each dose group. The remaining columns show the fraction of animals in each dose group that were found to have each tumor type at necropsy.

* Tumor incidence rates in bold and marked with an asterisk are significantly greater than in the control group ($p < 0.05$ by Fisher's Exact Test).

TABLE II: RESULTS ON BENZENE HEMATOTOXICIT9Y AND GENOTOXICITY

END POINT	RESULT	REFERENCE
Hematotoxicity in mouse bone marrow, measured by a variety of indicators	10 ppm x 8 weeks has no hematotoxic effect but 100 ppm x 1 week has a marked hematotoxic effect.	Farris *et al.,* 1997
Hematotoxicity in mouse bone marrow, indicated by changes in CFU-GM and spleen colony-forming unit (CFU-S) stem cell populations	10 ppm x 10 weeks has no myelotoxic effect in mice, but 100 ppm x 1 week greatly suppresses CFU-GM and CFU-S	Green *et al.,* 1981 a, b
Hematotoxicity in mouse bone marrow , measured by reduction in CFU-GM per tibia	21 ppm of benzene x 6 days (= 3,024 ppm-hours) had a *smaller* hematotoxic effect than 50 ppm	Toft *et al.,* 1982

bone marrow	x 2 days (2,400 ppm-hours).	
Hematotoxicity in mouse bone marrow , measured by reduction in CFU-GM per tibia bone marrow	95 ppm of benzene x 2 hr/day, 5 days/week x 2 weeks has little hematotoxic effect. Yet, 96 hours of continuous exposure to 21 ppm produces severe hematotoxicity. (Both are about 2000 ppm-hours)	Toft *et al.*, 1982
Hematotoxicity in mouse bone marrow, measured by erythropoiesis	Benzene metabolites (HQ and phenol) synergize strongly in suppressing murine erythropoiesis	Guy *et al*., 1990; Chen and Eastmond, 1994, 1995
Genotoxicity in mouse bone marrow erythrocytes, measured by induction of micronuclei in polychromatic erythrocytes (MN-PCE).	HQ and phenol synergize in creating micronuclei (MN) in erythrocytes	Chen and Eastmond, 1995; Barale *et al*., 1990; Marrazzini *et al*., 1994
Genotoxicity in human lymphocytes in vitro, measured by clastogenicity.	HQ and catechol synergize strongly (7 x additive effect) in creating genotoxic damage in cultured human lymphocytes	Robertson *et al*.,1991
Genotoxicity in mouse bone marrow erythrocytes, measured by MN-PCE.	MN-PCE response is insensitive to duration of exposure and follows a quadratic dose-response curve below 200 ppm.	Toft et al., 1982; Tice *et al.,* 1989, Luke et al., 1988b Farris *et al.,* 1996
Genotoxicity in mouse bone marrow *in vivo*, measured by chromosomal aberrations	Doubling administered dose from 440 to 880 mg/kg increases chromosomal aberrations 8-fold.	Ciranni *et al.,* 1991

TABLE III: DESIGN OF MODEL VALIDATION EXPERIMENT IN MICE

Group	1	2	3	4	5	6	7	8	9	10	11	12	13	14
0		X		x			x	x	x	x	x			x
1	D	X	x	x					x					
2	D		D, x	x			x	X		x	x			x
3	D		D				D, x	X	x	x	x			x

D = administration of dose (50 mg/kg via i.p. injection)

X = sacrifice of animals

TABLE IV: RECENT EVIDENCE ON CYTOTOXICITY AND DOSE-RESPONSE RELATIONS FOR SEVERAL CHEMICALS

CHEMICAL	MAIN RESULT	CONJECTURED MECHANISM	COMMENTS	REFERENCE
Benzene	"Excess risk due to benzene exposure may be nonexistent or negative at sufficiently low doses." PBPK and hematotoxic models both support this **nonlinear** pattern.	Benzene exposure may increase s-MDS/leukemia risk by cytotoxic action on HPC and normal stem cell populations followed by **compensating proliferation.**	A simulation model predicts that at low concentrations, benzene increases stem cell counts in the bone marrow, instead of reducing them.	Cox, 1996. See also Farris *et al.,* 1997 and Cronkite *et al.,* 1989.
Caffeic acid	Forestomach and kidney hyperplasia in rats and mice are **nonlinear** ("J-shaped or U-shaped") functions of dietary concentrations.	**Hyperplasia** is considered the probable cause of cancer in the two target organs (forestomach and kidney).		Lutz *et al.,*1997
Chloroform	"The dose-response relationship for chloroform-induced tumors in rats and mice is **nonlinear**" (J- or U-shaped)	Cytotoxicity leading to **regenerative cell proliferation** is "the likely mode of action for the carcinogenic effects of chloroform".	Chloroform lacks clear direct *in vivo* or *in vitro* genotoxicity.	Golden *et al.,* 1997. See also Butterworth *et al.,* 1994.
Diesel Exhaust	The dose-response relation for DE-induced lung tumors is **highly nonlinear** (with an apparent threshold or very steep J or U shape).	Lung tumors in rats occur only if exposures "over-burden" the lung, causing repetitive irritation/injury and **compensating cell proliferation.**		Valberg and Watson, 1996
Formalde-hyde	"Formaldehyde induces **nonlinear,** concentration-dependent… cell proliferation and DNA-protein cross-link formation." (Monticello and Morgan, 1994)	"The nonlinearity observed in formaldehyde-induced rodent nasal cancer is consistent with a high-concentration effect of **regenerative cell proliferation** …"	"The concentration-dependent increases in cell proliferation correlated strongly with the tumor response curve"	Monticello and Morgan, 1994. See also Monticello *et al.,* 1996 and Lutz, 1991.
TCE	"The mechanism of carcinogenesis of TCE… is **nonlinear:** very high doses, sufficient to cause cellular necrosis, are necessary."	"Malignancy arises from repeated cycles of necrosis and **regeneration with the ultimate emergence of hyperplasia** and then neoplasia."		Steinberg and DeSesso, 1993. See also Clewell *et al.,* 1995.

Figures, in order of appearance

FIGURE 1: MODEL PREDICTIONS *vs*. CLINICAL OBSERVATIONS FOR TWO ADMINISTERED DOSE HISTORIES

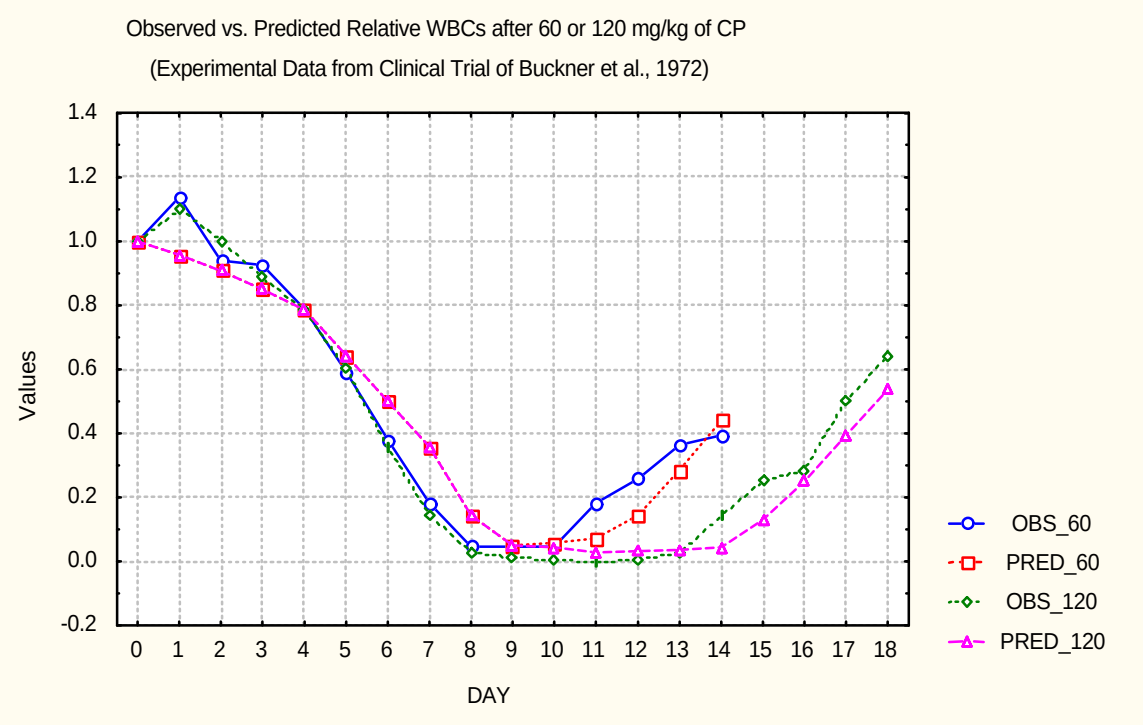

OBS = observed values; PRED = model-predicted values

FIGURE 2a: Predicted vs. Actual CFU-GM Values In Mice After One CP Injection

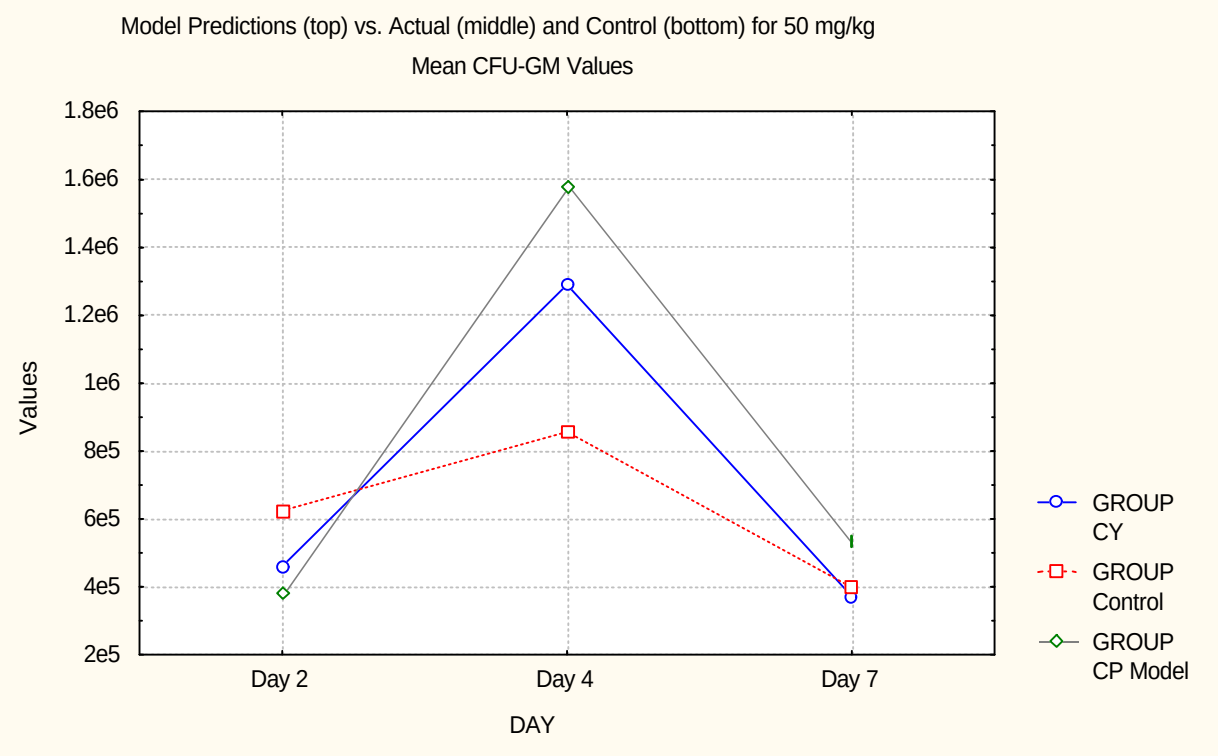

FIGURE 2b: Predicted vs. Actual CFU-GM Values In Mice After One, Two, and Three CP Injections

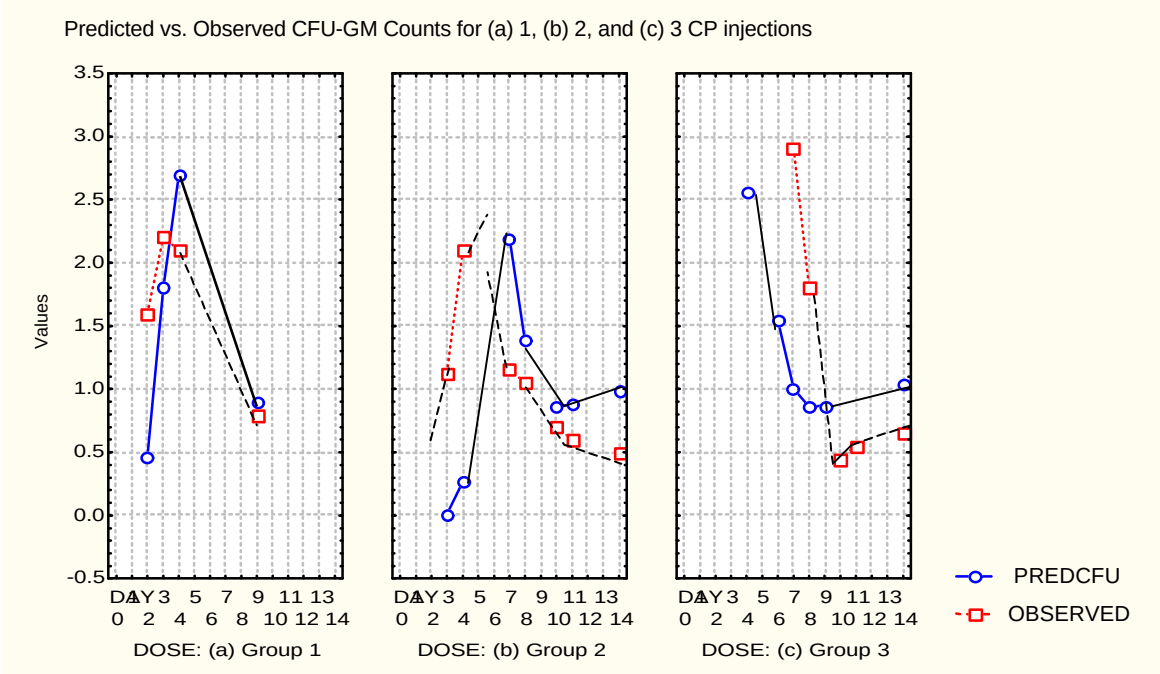

FIGURE 3: Equal Administered Doses may Create Different Hematotoxic Responses

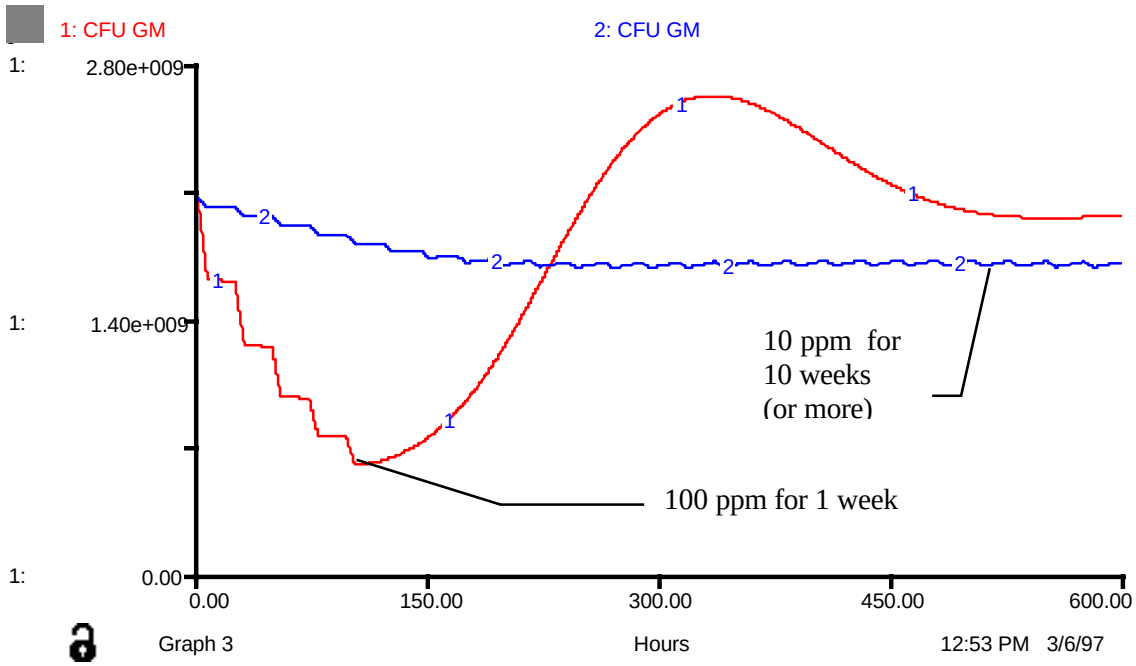

FIGURE 2: MODEL PREDICTIONS *vs*. CLINICAL OBSERVATIONS FOR A FOUR-DAY ADMINISTERED DOSE HISTORY

CFU-GM
time course in
Actual mice

FIGURE 3a: Predicted vs. Actual CFU-GM Values In Mice After One CP Injection

FIGURE 3b: Predicted vs. Actual CFU-GM Values In Mice After One, Two, and Three CP Injections

FIGURE 4: SHORT, HIGH-CONCENTRATION DOSING MAXIMIZES STEM CELL RESPONSE FOR A GIVEN TOTAL ADMINISTERED DOSE (AUC)

FIGURE 5: LONGER EXPOSURE PERIODS DO NOT CREATE PROPORTIONALLY GREATER RISKS

Explanation: This figure shows the effects on early CFU-GM stem cells (top panel) and peripheral WBCs (bottom panel) of applying the same concentration (AUC per day) for different amounts of time. Administering the dose over 480 hours instead of 48 hours leads to no deeper a nadir, but delays the post-exposure compensating proliferation.

Although the proliferation is more pronounced when it occurs, the initial nadir may not be deep enough to recruit many "immature" stem cells; moreover, the increased level of (presumably predominantly normal) stem cells in the interim and the increased opportunity for DNA repair and other damage control processes to operate may make the longer-duration exposure less hazardous. Even without these speculative hypotheses, the response of CFU-GM cells (e.g., nadir, zenith, AUC, etc.) for the 480-hour exposure are much less than 10 times as great as the corresponding responses for the 48-hour exposure

FIGURE 6: HEMATOPOIETIC RESPONSE IS A NONMONOTONIC FUNCTION OF CONCENTRATION IN SUSTAINED LOW-LEVEL INFUSIONS

Explanation: This figure shows the effects on early CFU-GM stem cells (top panel) and peripheral WBCs (bottom panel) of different administered dose concentrations sustained throughout the simulation. Hematopoietic responses such as the zenith, AUC, and stressed equilibrium levels of CFU-GM cells first increase and then decrease as a function of concentration. (This nonmonotonic pattern also occurs in finite-duration exposures.)

Explanation: This figure shows the effects on early CFU-GM stem cells (top panel) and peripheral WBCs (bottom panel) of different administered dose histories corresponding to the same total administered dose (AUC). Administering the dose over 8 hours instead of 480 hours leads to a deeper nadir followed more immediately by a more extensive proliferation. According to the hypothesized model of leukemogenesis described in Section 4, this response pattern maximizes leukemia risk.